J/ψ Absorption in Heavy Ion Collisions II

L. Maiani[*]

Università di Roma 'La Sapienza', Roma, Italy; I.N.F.N., Sezione di Roma, Roma, Italy

F. Piccinini[†]

I.N.F.N. Sezione di Pavia and Dipartimento di Fisica Nucleare e Teorica, via A. Bassi 6, I-27100 Pavia, Italy

A.D. Polosa[‡]

Centro Studi e Ricerche "E. Fermi", via Panisperna 89/A-00184, Roma, Italy

V. Riquer[§]

CERN, Department of Physics, Theory Division, Geneva, Switzerland
(Dated: February 2, 2008)

Using the methods introduced in a previous paper, we consider the dissociation of J/ψ by the lowest-lying pseudoscalar and vector mesons in the hadronic fireball formed in heavy ion collisions, assumed to be a hadron gas at temperature T. Absorption by nuclear matter is accounted for as well. We compare with the S-U and Pb-Pb data presented by the NA50 Collaboration. From data at low centrality we find $T = 165 - 185$ MeV, close to the predicted temperature of the transition to quark-gluon plasma and to the temperatures measured by hadron abundances. We extrapolate to higher centralities with the approximation of scaling the energy density of the fireball with the average baryon density per unit transverse area. Using the energy-temperature relation of the hadron gas made by the same pseudoscalar and vector mesons, the fall off of J/ψ production shown by the NA50 data can be marginally reproduced only for the highest temperature, $T = 185$ MeV. If we use the energy-temperature relation of a Hagedorn gas with limiting temperature $T_H = 177$ MeV, predictions fall short from reproducing the data. These results suggest that a different mechanism is responsible for the J/ψ suppression at large centralities, which could very well be the formation of quark-gluon plasma.

PACS numbers: 25.75.-q, 12.39.-x

I. INTRODUCTION

In a recent paper [1] we have presented a theoretical study of the dissociation cross-section $\pi + J/\psi \to D^{(*)} + \bar{D}^{(*)}$ to analyze the absorption of J/ψ in heavy ion collisions. The disappearance of the J/ψ's created in the early stages of the collision was considered as mainly due to two subsequent processes:

1. The interactions of J/ψ with the nuclear medium traversed during the interpenetration of the two heavy nuclei, with an absorption cross section per nucleon experimentally determined [2] from the inclusive J/ψ production in $p + A$ collisions;

2. The dissociation process: $\pi + J/\psi \to D^{(*)} + \bar{D}^{(*)}$ induced by the pions of the hadron gas formed in the heavy-ion collision, the so-called co-moving particles [3].

In [1] the absorption curves thus obtained have been compared to a data analysis by the NA50 collaboration [4]. Fitting the data at low centrality we found a value for the inner temperature of the pion gas of about $T = 225 \pm 15$ MeV. Extrapolation of the absorption curve at large centrality was done by assuming an increase of the energy density deposited in the fireball proportional to the average number of nucleons per unit of overlapping area [3], a quantity which increases with decreasing impact parameter. The results did not seem to reproduce the fast increase of absorption observed by NA50, thus lending some support to the idea that in large centrality collisions a quark-gluon plasma phase is produced, which would impair the formation of the J/ψ because of QCD Debye screening [5]. As already noted in [1], however, for this method of analysis to be accurate one should go beyond the approximation of

a simple pion gas and consider the more realistic case in which further particles/resonances appear in the fireball at thermal equilibrium, which can appreciably contribute to J/ψ dissociation.

In the present paper, we extend our previous work in several directions. First, we include the J/ψ dissociation cross sections by the lowest lying pseudoscalar and vector mesons (Sect. II). We use the Constituent Quark Model (CQM) [6] as before, with couplings computed with flavour SU(3) symmetry, and nonet symmetry for the vector mesons. Real particle masses are used for reaction thresholds and to compute particle abundances in the hadron gas.

After defining the different lengths that characterize the collision (Sect. III), the absorption lengths vs. temperature are computed in the heath bath made by the hadron gas of pseudoscalar and vector mesons at a given temperature T (Sect. IV). Not unexpectedly [7], the largest correction to the pion gas situation is due to the vector mesons. Notwithstanding the considerably larger mass, they contribute to J/ψ absorption about as much as pions, for two reasons: (i) dissociation reactions have very low or no threshold, thus making all particles useful as opposed to pions, which are effective only above a relatively high-energy threshold; (ii) the large spin and flavour multiplicities (a factor of 24 with respect to 3 for pions, for the complex $\rho + \omega + K^* + \bar{K}^*$).

The total inverse absorption length, $\Sigma_i \langle \rho_i \sigma_i \rangle_T$, is considerably increased with respect to the pure pion gas. Correspondingly, we find a substantial decrease in the estimated temperature of the fireball in low centrality collisions, which turns out to be now in the range $165 - 185$ MeV (see Fig. 7). Extrapolation to higher centrality is done using the relation between energy density and temperature appropriate to the hadron gas we are considering and it leads to increasing temperatures with increasing centrality up to $180 - 200$ MeV at zero impact parameter, $l = 2R = 13$ fm for Pb (l is the linear size of the fireball and R the nuclear radius). The corresponding hardening of the attenuation curves, however, do not really reproduce the falling of J/ψ production in this region, as shown by Fig. 7, supporting the idea of a change of regime, this time in a more realistic region of the thermodinamical parameters with respect to [1].

In the range of temperatures we have found, one expects to deal with a hadron gas of increasing complexity approaching the Hagedorn gas [8], with an infinite number of resonances and a level density exponentially increasing with mass. This situation is known to give rise to a limiting temperature [9], which was interpreted in [10] as the temperature at which the transition to a quark-gluon plasma phase starts to take place. In Sect. V, starting from the fit at low centrality, we extrapolate to higher centrality with the energy-temperature relation appropriate to the Hagedorn gas, with a Hagedorn temperature $T_H = 177$ MeV. This temperature is consistent with the transition temperature estimated in QCD lattice calculations [11], with the empirical density of hadron levels up to 2 GeV, as estimated by [9], and with the temperatures determined at SPS and RHIC from particles relative abundances at freeze-out [12]. We find that the increase of the energy deposited in the collision does not lead anymore to an increase of temperature, hence of the opacity: the extra energy deposited in the fireball for increasing centrality goes into an increase of the thermodinamical degrees of freedom, which ultimately should lead to the phase transition.

The curve corresponding to the absorption by the Hagedorn gas falls definitely short to explain the further decrease of J/ψ abundance, as observed by NA50. It is tempting to interpret the discrepancy shown in Fig. 8 as a signal of quark-gluon plasma formation. However, caution is required, due to the unavoidable truncation we have made in the calculation of the opacities. While higher resonances are expected to contribute less and less, their cumulative effect could resum to a large contribution to the dissociation cross-section and lead to an increase in opacity even for the very small temperature increases allowed by the vicinity of the limiting temperature.

Sect. VI contains conclusions and outlook. We find it very satisfactory that a microscopic calculation based on the CQM and the observed opacities produce values of the temperature that are consistent with the measured freeze-out temperature in ion collisions and are just at the border of the transition temperature predicted by QCD lattice calculation and by the Hagedorn hadron gas. A point borne out clearly by our analysis is that the picture would be considerably more clear if the relative normalization of S-U vs. Pb-Pb data was better understood [13]. In this respect, further measurements at low energy, aimed at resolving the experimental issue of the relative normalization, could be very useful.

All in all, the results shown in Figs. 7 (a),(b) or, even more, in Fig. 8 are quite impressive. They seem to us very suggestive that a new mechanism to suppress J/ψ is setting in at large centralities. This could very well be the formation of quark gluon plasma. It would be extremely important to correlate other signals to the present one, in order to get to a definite conclusion about the presence of a phase transition.

In this paper we correct few mistakes which affected our analysis in [1]. The pion cross sections presented here supersede those in [1], where we found a trivial numerical mistake; the average lenght traversed by the J/ψ in the fireball was incorrectly estimated to be $(6/10)l$ rather than $(3/8)l$. All together these corrections would increase the temperature given in [1] by $15 - 20$ MeV, leaving all conclusions unchanged. Finally, a misprint led to the factor $2\pi/3$ in Eq. (13) of Ref. [1], to be replaced by $\pi/2$.

II. CROSS SECTION COMPUTATIONS

The evaluation of the cross sections for the processes $(\pi, \eta, K, \rho, \omega, K^*, \phi) + J/\psi \rightarrow D_{(s)}^{(*)} D_{(s)}^{(*)}$ proceeds through the computation of diagrams very similar to those listed in [1]. Such tree level diagrams involve effective tri-linear $g_3 = (\pi, \eta, K, \rho, ...) D_{(s)}^{(*)} D_{(s)}^{(*)}$ or $g_3 = J/\psi D_{(s)}^{(*)} D_{(s)}^{(*)}$ and four-linear $g_4 = (\pi, \eta, K, \rho, ...) J/\psi D_{(s)}^{(*)} D_{(s)}^{(*)}$ couplings which we can estimate using the CQM model, originally devised to compute exclusive heavy-light meson decays and tested on a quite large number of such processes [6].

CQM is based on an effective Lagrangian which incorporates the heavy quark spin-flavor symmetries and the chiral symmetry in the light sector. In particular, it contains effective vertices between a heavy meson and its constituent quarks (see the vertices in l.h.s. of Fig. 1) whose emergence has been shown to occur when applying bosonization techniques to Nambu-Jona-Lasinio interaction terms of heavy and light quark fields [14]. On this basis we believe that CQM is a more solid approach to the computation of g_3, g_4 if compared to the various methods available in the literature, often based on SU(4) symmetry (for a review see e.g. [15]).
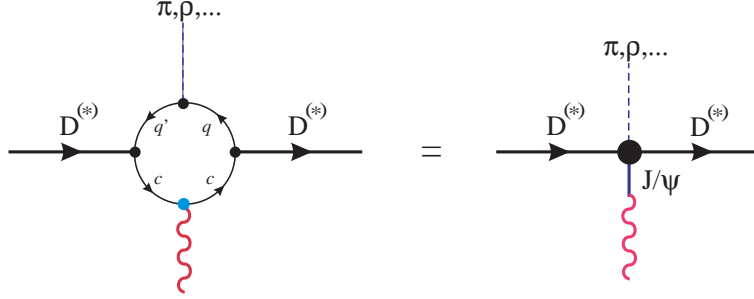

FIG. 1: Basic diagrammatic equation to compute g_3 and g_4 couplings.

In Fig. 1 we show the typical equation which has to be solved in order to obtain $g_4(g_3)$ in the various cases at hand: on the r.h.s. we represent the effective four-linear couplings to be used in the cross section calculation (to obtain the tri-linear coupling we suppress either the J/ψ line or the dashed line of the light particles); the effective interaction at the meson level (r.h.s.) is modeled as an interaction at the quark-meson level (l.h.s. of Fig. 1).

The J/ψ is introduced using a Vector Meson Dominance (VMD) Ansatz: in the effective loop on the l.h.s. of Fig. 1 we have a vector current insertion on the heavy quark line c while on the r.h.s. the J/ψ is assumed to dominate the tower of $J^{PC} = 1^{--}$, $c\bar{c}$ states mixing with the vector current (for more details see [16]). Similarly, vector particles coupled to the light quark component of the heavy mesons ρ, ω, when $q = (u, d)$, or K^*, ϕ, when one or both light quarks are $q = s$, are also taken into account using VMD arguments. The pion and other pseudoscalar fields have a derivative coupling to the light quarks of the Georgi-Manohar kind [17].

Once established the form of the effective vertices occurring in the loop diagram on the l.h.s. of Fig. 1, one has just to compute it. The momenta running in the loop are limited by two Schwinger cut-off's: one in the ultraviolet and one in the infrared. The ultraviolet cut-off Λ has been set to the chiral expansion scale $\Lambda_\chi \simeq 4\pi f_\pi$ while the infrared μ prevents loop momenta to access the confinement energy region (CQM does not include any confining potential). To give a flavor of the kind of calculations involved, consider that the loop integral for the four-linear coupling $\rho J/\psi D^{(*)} D^{(*)}$ is written as follows:

$$(-1)\sqrt{Z_H m_H Z_{H'} m_{H'}} \times N_c \int \frac{d^4 l}{(2\pi)^4 i} \times$$
$$\text{Tr}\left[(-i\bar{H}'(v'))\frac{1}{v' \cdot l + \Delta}(i\frac{m_J^2}{f_J}\slashed{\eta})\frac{1}{v \cdot l + \Delta}(-iH(v))\frac{1}{\slashed{l} - m}(i\frac{m_\rho^2}{f_\rho}\slashed{\epsilon})\frac{1}{\slashed{l} + \slashed{q} - m}\right], \tag{1}$$

where H and $\bar{H}'$ represent the heavy-light external meson fields labeled by their four-velocities v, v'; the Feynman rules for their couplings to constituent quarks, in this case the $\sqrt{Z_H m_H Z_{H'} m_{H'}}$ coupling factor, are discussed in [6]. The heavy quark propagators (those obtained by the standard Dirac propagator in the limit of very heavy $Q = b, c$ mass) are also labeled by v, v' while we have the usual expression for the light propagators. The parameter Δ appearing in the heavy propagator is defined to be $\Delta = M_H - m_Q$, the mass of the heavy-light meson minus the mass of the heavy quark contained in it. Δ is the the main free parameter of the model. It varies in the range $\Delta = 0.3 - 0.5$ GeV for u, d light quarks and $0.5 - 0.7$ GeV for strange quarks [18]. Varying Δ allows to estimate the theoretical error.

The ρ is coupled via its VMD coupling to the light quarks, ϵ being its polarization. The J/ψ, with polarization η, is also coupled via VMD to the heavy quarks (η appears in the trace between two heavy quark propagators, ϵ appears between two light quark propagators). In front of this expression we have the fermion loop factor.

The way to regularize and compute such integrals is discussed in [19]. The trace computation in (1) will introduce a number of scalar combinations of the momenta and polarizations of the external particles. Each of these combinations will be weighted by a scalar integral which amounts to a numerical factor: what we call the coupling. Actually such scalar integrals depend on the energy of the ρ. In general the expressions obtained in the $\sigma_{\rho J/\psi}$ computation appear to be quite complicated functions of E_ρ if compared to those obtained when studying only J/ψ interactions with pions [16]. On the other hand, having in mind a hadron gas at a temperature $T \approx 170$ MeV, we restrict our study to the low energy interval $E_\rho \simeq 770 - 1000$ MeV and rely on the fact that the Boltzmann factor $\exp(-E/T)$ will cut off the high energy tails and work as a high energy form factor in the thermal averages $\langle \rho\sigma \rangle_T$ (we have explicitly tested that this occurs).

The couplings $\rho D^{(*)} D^{(*)}$, are computed in the same framework by simply dropping the J/ψ line in the diagrammatic equation of Fig. 1, as mentioned above.

The ω particle contribution is introduced in the thermal average by simply multiplying the ρ cross-section by a factor of $4/3$ (nonet symmetry). The amplitudes for K^* are deduced from those of the ρ by SU(3) symmetry. However, computing the K^* cross-sections, where a D_s meson will be produced in the final state, we take into account exact masses and thresholds. Similarly η and K contributions are computed by SU(3) symmetry from the pion couplings [16] but accounting for different kinematical thresholds. The calculation of the ϕ contribution is performed by replacing the constituent light quark mass, $m = 300$ MeV for $q = (u, d)$, with a constituent strange quark mass $m = 500$ MeV. Such an operation requires accordingly the modification of the Z_H couplings (see Eq. (1)) and of the infrared cutoff, as described in [18].

The final results for $\sigma_{\pi J/\psi}$ and $\sigma_{\rho J/\psi}$ are displayed in Fig. 2. We give the cross sections for π^+ and ρ^+.
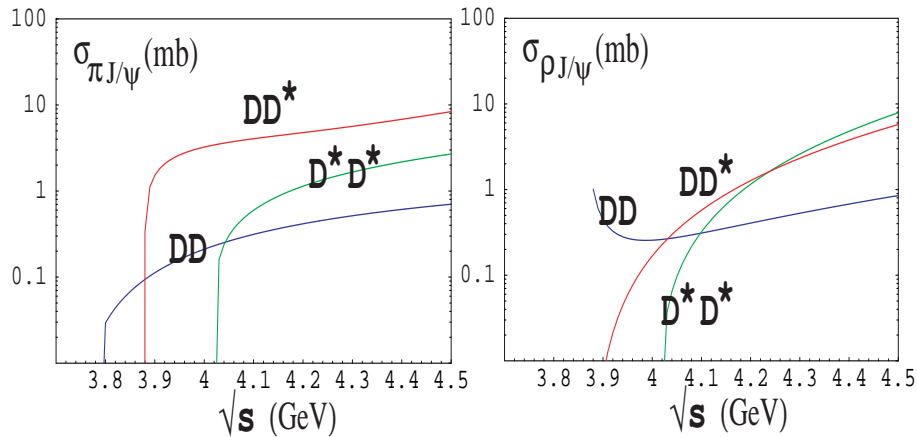

FIG. 2: The cross sections for the processes $(\pi^+, \rho^+) + J/\psi \to D^{(*)} \bar{D}^{(*)}$ versus energy.

III.   THE GEOMETRY OF THE COLLISIONS

The geometry of the heavy ion collision is shown schematically in Fig. 3, which depicts the time-evolution in the center of mass frame.

The impact parameter, b, is defined, as usual, as the transverse distance of the centers of the two nuclei. We consider the J/ψ to be created with Feynman's $x \approx 0$, during the overlap of the two nuclei. These particles have to overcome absorption from the column density of nucleons. In the center of mass frame the length of the column is L/γ. In the same frame, the density of nucleons is $\rho_{\text{nucl.}} \cdot \gamma$, so that the absorption factor is Lorentz invariant and given by $\exp(-\rho_{\text{nucl.}}\sigma_{\text{nucl.}}L)$. This is the same formula used in Ref. [4]. $\sigma_{\text{nucl.}}$, the nuclear absorption cross-section, has been determined by NA50 from the behaviour of the cross-section of $p + A \to J/\psi +$ anything as function of A. We take from Ref. [2]:

$$\sigma_{\text{nucl.}} = 4.3 \pm 0.3 \text{ mb} \tag{2}$$

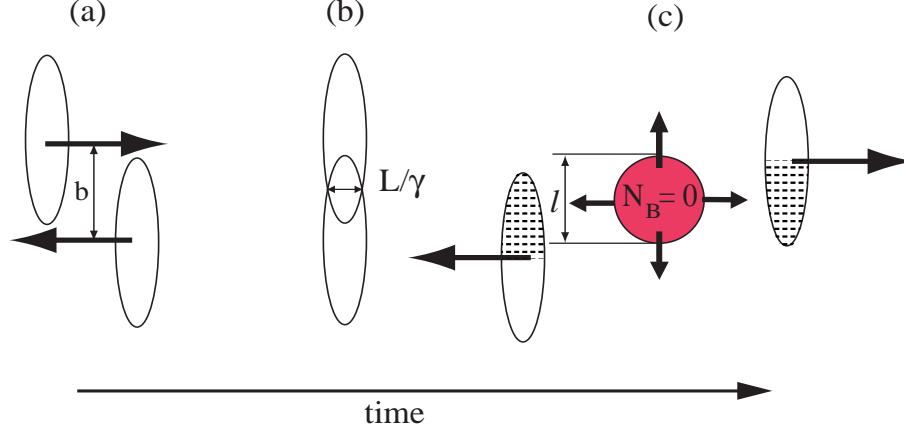$$\rho_{\text{nucl.}} = 0.17 \text{ fm}^{-3}. \tag{3}$$

FIG. 3: Time evolution of the collision of two heavy nuclei seen in the c.o.m. frame. A fireball with baryon number $N_B = 0$ is left behind the two receding nuclei. The fireball is expected to thermalize at the temperature T. The nucleons belonging to the nuclear overlapping regions fly apart as unbounded particles. The dimensions L/γ and l are respectively the linear dimension of the nuclear column the J/ψ has to traverse during the interpenetration of the two nuclei and the linear size of the fireball.

After collision, nuclear matter appears in part as a cloud of free (wounded) nucleons from the initially overlapping parts of the nuclei, represented as dotted regions in Fig. 3 (c), in part as forward going fragments from the non overlapping regions. The NA50 Collaboration has installed a Zero-Degree-Calorimeter (ZDC) which measures the energy of the forward going fragments, proportional to their nucleon number and therefore to their size, thereby determining the value of the impact parameter, b, for each collision [4]. The relation between L and b has been given in [20] in the framework of the Glauber theory.

In Fig. 3 we show the hadron fireball produced by the central collisions of the interacting nucleons [3] (the *comoving particles*). The fireball has a transverse dimension, l, approximately equal to the length of the overlapping region:

$$l = 2R - b, \tag{4}$$

where R is the nuclear radius. If we take, for simplicity, a spherical fireball, the average length that a J/ψ has to traverse before leaving it is $(3/8)l$, so that the attenuation factor due to absorption by the comoving particles is:

$$A_{\text{comoving}} \propto \exp\left[-\Sigma_i \langle \rho_i \sigma_i \rangle \frac{3}{8} l\right], \tag{5}$$

the subscript i labels the species of hadrons making up the fireball, ρ_i the number density of the effective (i.e. above threshold) particles and σ_i the corresponding J/ψ dissociation cross-section. Brackets indicate an average over the energy distribution in the fireball. As noted before, we can express the nuclear absorption length, L, as a function of b [20] and therefore, using (4), as a function of l. Putting all together, we write the attenuation of the J/ψ as a function of l according to:

$$A = N \times \exp[-\rho_{\text{nucl.}} \sigma_{\text{nucl.}} L(l)] \times \exp\left[-\Sigma_i \langle \rho_i \sigma_i \rangle \frac{3}{8} l\right], \tag{6}$$

where N is an appropriate normalization constant. As discussed in Ref. [3], the energy density deposited in the fireball is proportional to the average flux of nucleons participating to the collision, i.e., the number of nucleons per unit transverse area. This quantity increases with decreasing impact parameter. A simple estimate of the ratio of the energy density for two different values of b was given in [1] according to:

$$\frac{\epsilon(b_2/R)}{\epsilon(b_1/R)} = \frac{g(b_2/R)}{g(b_1/R)}, \tag{7}$$

with the geometrical factor $g(b/R)$ given by [1]:

$$g(b/R) = \frac{\pi}{2} \frac{(1 - b/2R)^2(1 + b/4R)}{\arccos(b/2R) - (b/2R)\sqrt{1 - b^2/4R^2}}. \tag{8}$$

IV. THERMAL AVERAGES AND ABSORPTION IN THE RESONANCE GAS

The fireball depicted in Fig. 3 (c) is expected to quickly thermalize (see [3]), giving rise, at least for low centrality collisions, to a hadron gas at temperature T. The thermalisation hypothesis is supported by the data from SPS and RHIC which show abundances and momenta distributions at freeze-out compatible with a temperature $T = 170 - 180$ MeV, see e.g. Ref. [9] and Ref. [12] for a review of recent data.

In Ref. [1] we have assumed the thermalised fireball to be a pion gas. We consider now a more general case of a boson gas made by the lowest-lying pseudoscalar and vector mesons, retaining, for simplicity, the assumption of vanishing chemical potential. What matters, for our considerations, are particle densities above the dissociation threshold. Assuming the J/ψ to be at rest, this means particles with energy larger than $E_{\text{th.}}$:

$$E_{\text{th.}} = \frac{(M_{fin})^2 - (M_{J/\psi})^2 - m^2}{2M_{J/\psi}};$$ (9)

m is the projectile particle mass and M_{fin} the sum of the final particles masses. Explicitly, we have:

$$\rho(T) = \frac{N}{2\pi^2} \int_{E_{\text{th.}}}^{\infty} dE \frac{pE}{e^{E/kT} - 1}.$$ (10)

N is the total multiplicity (spin times charge, $N = 3, 9$ for pion and for ρ, respectively) and $p = \sqrt{E^2 - m^2}$. We report in Fig. 4 and in Tables I and II the number densities above threshold for the particles considered. In Table I, we give in parenthesis the total number density of pions as well.
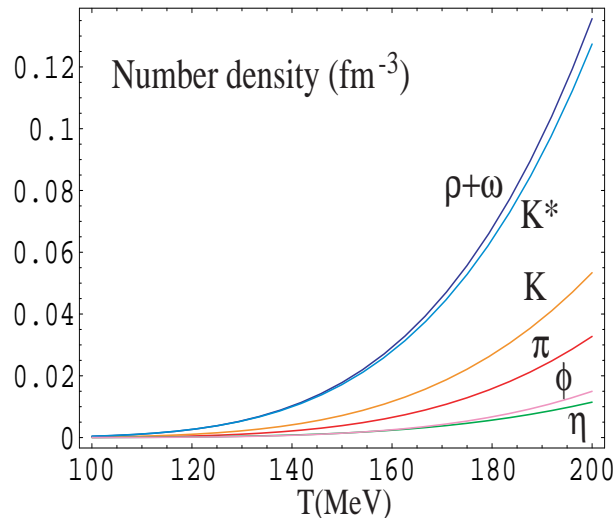

FIG. 4: Number densities of the hadron gas particles h being above the kinematical threshold for the $hJ/\psi \to D^{(*)}_{(s)} \bar{D}^{(*)}_{(s)}$ reaction.

The energy density associated to the various particles are listed in Tables III to V. In this case the sum over the full energy range is understood:

$$\epsilon(T) = \frac{N}{2\pi^2} \int_{m}^{\infty} dE \frac{pE^2}{e^{E/kT} - 1}.$$ (11)

The contribution of the other particles is not at all negligible with respect to pions, even at temperatures as low as $T = 150$ MeV, [9], particularly in terms of the energy density.

We report in Figs. 5 (a,b) the energy densities divided by $\epsilon_0 = T^4 \pi^2 / 30$. The ratio, g, gives the effective number of degrees of freedom which are active at the particular temperature. Pions give $g = 3$ already at $T = 150$ MeV (Fig. 5 (a)), which is increased to $g = 7 - 10$ by the other particles, for $T = 150 - 180$ MeV. In Fig. 5 (b) we specify the contributions of the different particles, with Kaons ($N = 4$) and the lowest lying vector mesons, ρ and ω ($N = 12$) providing the dominant contributions.
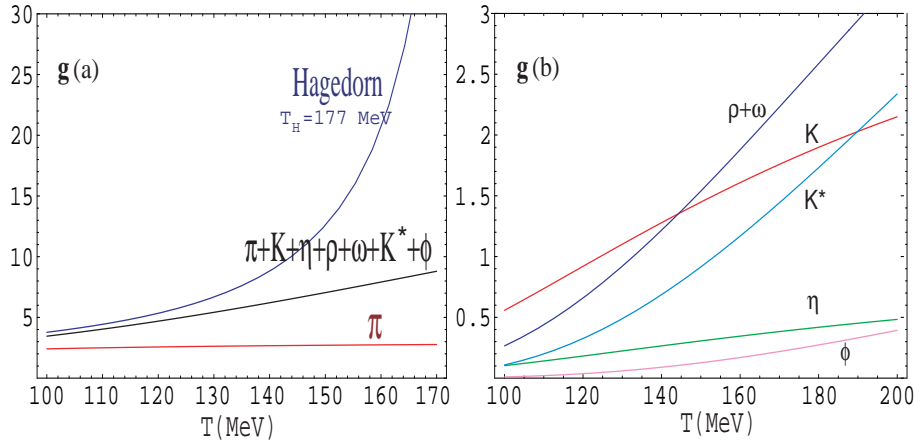
FIG. 5: The effective number of degrees of freedom g active at a particular temperature. In panel (a) we show the dramatic increase of g for the Hagedorn gas with limiting temperature $T_H = 177$ MeV, see (15). In panel (b) we specify the contribution of the different components of the hadron gas.

Thermal averages of the product $\rho \cdot \sigma$ give the inverse of the absorption length due to each particle species, x, and are done with analogous formulae:

$$\langle \rho \cdot \sigma_{x+J/\psi \to D^{(*)} \bar{D}^{(*)}} \rangle_T = \frac{N}{2\pi^2} \int_{E_{\text{th.}}}^{\infty} dE \, \frac{pE\sigma(E)}{e^{E/kT} - 1}. \tag{12}$$

We give the values of the inverse absorption lengths as function of temperatures in Table V and Fig. 6. ρ and ω give larger contributions than the pions. This is due to the absence of threshold in the dissociation reaction, which makes particles of all energies to be effective, and to the large multiplicity.
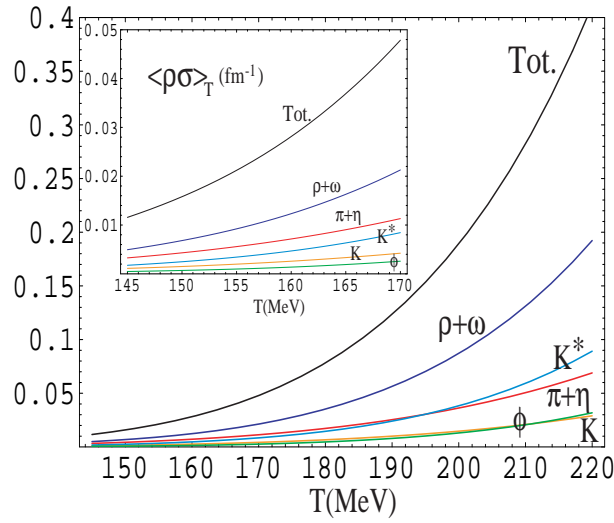

FIG. 6: The inverse absorption lengths as a function of temperature.

The absorption lengths thus computed are inserted in the absorption master formula (6). We compare in Fig. 7, the absorption curves thus obtained with the NA50 data in S-U and Pb-Pb collisions, for $T = 165 - 185$ MeV [21]. The normalization constant in (6) is chosen to fit the data around $l = 3$ fm. The data for $l \leq 4$ fm favour temperatures of this order. In the same figure, we show the curve corresponding to the pure nuclear absorption.

To extrapolate to higher centralities, we keep into account the increase in the energy density deposited in the collision as explained in Sect. III. The increase in temperature for increasing centrality makes the absorption to

increase, as shown in Fig. 7 (b), with respect to Fig. 7 (a) where the geometrical effect is neglected. In Fig. 7 (b) we label the curves with the value of the temperature at $l = 3.4$ fm; the temperature increases along the curves, up to $T \approx 180 - 200$ MeV for $l = 11$ fm.
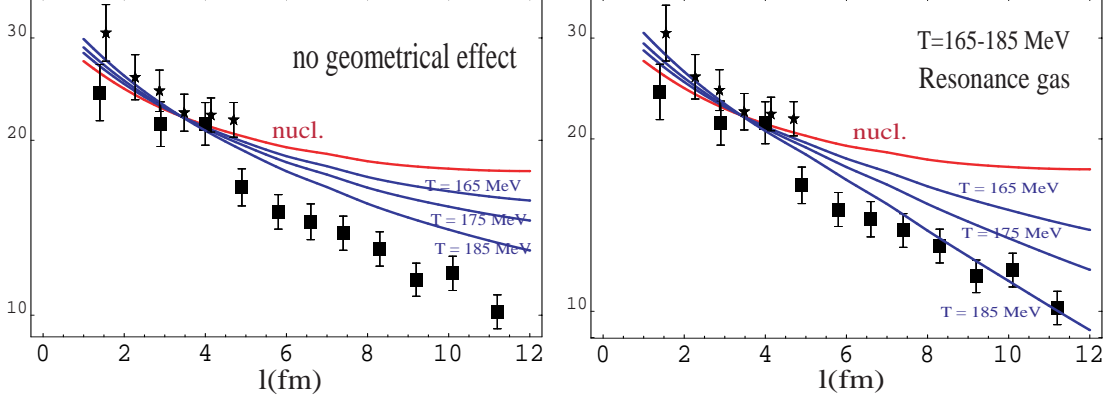

FIG. 7: The absorption curves are compared to the most recent data analysis of the J/ψ yield in S-U (star) and Pb-Pb (box) collisions [13]. Left panel: the absorption by comoving particles is described by a single temperature; the effect of nuclear absorption alone is shown by the upper curve (since the relation between L and l is non-linear, the nuclear absorption does not give rise to a simple exponential, unlike the isothermal absorption by comoving particles). Right panel: the temperature increase due to the geometrical effect described in Sect. III is accounted for with the energy-temperature relation of the hadron gas. The temperatures indicated refer to $l = 3.4$ fm.

The inclusion of the lowest lying resonances improves greatly the consistency of the whole picture, bringing the estimated temperatures below the temperature expected for the phase transition and closer to the temperatures measured at freeze-out, from the abundances of the different hadrons. The curve labeled with $T = 175$ MeV, which has T varying from 175 to about 190 MeV, fits well the data for low centrality but still falls short from reproducing the observed drop in the production of the J/ψ above, say, $l = 5$ fm. The curve with initial temperature $T = 185$ MeV fits the low centrality data as well and follows closer the data at large centrality. However the temperature exceeds 200 MeV at $l \simeq 11$ fm which is likely too a high value for a hadron gas (see next Section).

The increase in temperature due to the increase in energy density that we find is definitely less pronounced than what found for the pion gas in [1]. The reason is that in the resonance gas the number of degrees of freedom increases appreciably with temperature. The extra energy density provided has to be shared among more and more degrees of freedom and the temperature increases less than with a fixed $\epsilon = CT^4$ power law. This behaviour begins to reproduce what is expected in the case of a Hagedorn gas, with an exponentially increasing density of resonances per unit interval of mass [8],[9],[10], which we turn now to consider.

T (MeV)	ρ^π (ρ^π_{Tot}) (fm^{-3})	ρ^η (fm^{-3})	ρ^K (fm^{-3})	$\langle\rho\sigma\rangle_T^{\pi+\eta}$ (fm^{-1})	$\langle\rho\sigma\rangle_T^K$ (fm^{-1})
150	0.004 (0.12)	0.001	0.006	0.004	0.001
165	0.008 (0.17)	0.003	0.012	0.009	0.003
180	0.016 (0.22)	0.006	0.022	0.017	0.007
195	0.028 (0.29)	0.010	0.039	0.030	0.012
210	0.045 (0.37)	0.016	0.062	0.050	0.021
225	0.069 (0.47)	0.024	0.095	0.080	0.034
240	0.102 (0.57)	0.035	0.139	0.121	0.052

TABLE I: Number densities and inverse absorption lengths for the pseudoscalar particles in the gas. The number densities are relative to those particles which are over the kinematical threshold to open the $D^{(*)}_{(s)} \bar{D}^{(*)}_{(s)}$ channel. In the case of pions, we report in parenthesis their total number density (i.e., the one including pions below threshold).

T (MeV)	$\rho^{\rho+\omega}$ (fm^{-3})	ρ^{K^*} (fm^{-3})	ρ^{ϕ} (fm^{-3})	$\langle\rho\sigma\rangle_T^{\rho+\omega}$ (fm^{-1})	$\langle\rho\sigma\rangle_T^{K^*}$ (fm^{-1})	$\langle\rho\sigma\rangle_T^{\phi}$ (fm^{-1})
150	0.018	0.017	0.001	0.007	0.002	0.0007
165	0.037	0.035	0.003	0.016	0.006	0.002
180	0.068	0.064	0.007	0.035	0.014	0.005
195	0.115	0.108	0.012	0.070	0.030	0.010
210	0.184	0.172	0.021	0.131	0.059	0.020
225	0.279	0.260	0.034	0.231	0.108	0.039
240	0.404	0.377	0.052	0.388	0.188	0.070

TABLE II: Same as Table I for vector particles.

T (MeV)	ϵ^{π} (MeV/fm^{-3})	ϵ^{η} (MeV/fm^{-3})	ϵ^{K} (MeV/fm^{-3})
150	58.8	6.6	31.4
165	87.5	11.5	53.5
180	125.5	18.8	85.3
195	175	28.9	129
210	237	42.6	188
225	314	60.6	265
240	409	83.6	362

TABLE III: Energy density for the pseudoscalar particles in the gas.

V.   ABSORPTION IN A HAGEDORN GAS

In the range of temperatures we have found, one expects to deal with a hadron gas of increasing complexity, approaching the Hagedorn gas [8], which has an infinite number of resonances with a level density exponentially increasing with mass. This situation gives rise to a limiting temperature [9], the Hagedorn temperature T_H, which was interpreted in [10] as the temperature at which the transition to a quark-gluon plasma phase starts to take place. The Hagedorn temperature can be estimated from a fit to the resonance level density below 2 GeV, appropriately smeared down in the lowest end. In [9] a value $T_H = 158$ MeV is estimated. However, this value is lower than the observed hadron temperature at freeze-out and also lower than the estimates of the transition temperature from lattice QCD calculations, see Ref. [11]. As a reasonable compromise, we take $T_H = 177$ MeV, which still fits the resonance spectrum and it agrees with lattice QCD calculations and with the observed freeze-out temperature. We use the partition function of the Hagedorn gas in the form [9]:

$$\ln(Z_H) = V\left(\frac{T}{2\pi}\right)^{3/2}\int_0^\infty \rho(m)e^{-m/T}dm = V\left(\frac{T}{2\pi}\right)^{3/2}\int_0^\infty C\frac{1}{(m_0^2+m^2)^{3/2}}e^{m/T_H}e^{-m/T}dm, \tag{13}$$

with [22]:

$$C = 2.12 \text{ GeV}^2; \qquad m_0 = 0.96 \text{ GeV}; \qquad T_H = 177 \text{ MeV} \tag{14}$$

and the energy density ($\beta = 1/T$):

$$\epsilon = -\frac{\partial}{\partial\beta}\ln Z_H + \epsilon_\pi(T). \tag{15}$$

To get the total energy density we have added the contribution of the pion, Eq. (11) which is not included in $\rho(m)$. The number of effective degrees of freedom vs. temperature is shown in Fig. 5.

To make a numerical calculation possible, we have to make an assumption on the J/ψ dissociation cross-section by the hadron resonances. We assume that only the pseudoscalar and the vector mesons we have considered before are relevant to dissociate the J/ψ. Starting from the results of Fig. 7, we extrapolate to increasing centrality using the energy-temperature relation of the Hagedorn gas. This is shown in Fig. 8, using as initial temperature $T = 175$ MeV. The result is quite spectacular. The sharp rise of the degrees of freedom due to the vicinity of the Hagedorn temperature makes so that the temperature of the gas practically does not rise at all, the dissociation curve cannot become harder, and the prediction falls really short from explaining the drop observed by NA50. The simplest interpretation of

T (MeV)	$\epsilon^{\rho+\omega}$ (MeV/fm^{-3})	ϵ^{K^*} (MeV/fm^{-3})	ϵ^{ϕ} (MeV/fm^{-3})
150	33.4	31.4	2.7
165	65.2	53.5	6.1
180	116	85.3	12.3
195	193	129	22.4
210	304	188	38.0
225	455	265	61.0
240	657	362	93.4

TABLE IV: Energy density for the vector particles in the gas.

T (MeV)	ρ^{Tot} fm^{-3}	$\langle \rho\sigma \rangle_T^{Tot}$ (fm^{-1})	ϵ^{Tot} (MeV/fm^{-3})	g
150	0.050	0.016	153	7.3
165	0.1	0.037	265	8.7
180	0.18	0.078	436	10.0
195	0.32	0.153	684	11.4
210	0.51	0.282	1030	12.9
225	0.77	0.492	1497	14.2
240	1.13	0.821	2112	15.5

TABLE V: Total number densities, inverse absorption lengths, energy densities and number of active degrees of freedom, summed over the various components of the hadron gas.

Fig. 8 is that with increasing centrality, more energy is deposited but this goes into the excitation of more and more thermodinamical degrees of freedom leading to the final transition in the quark-gluon plasma. The curve shown in the figure would represent the limiting absorption from a hadron gas, anything harder being due to the dissociation of the J/ψ in the quark-gluon plasma phase.

Some words of caution are in order. In the framework of the CQM, it is certainly reasonable to expect the relevant insertions in the quark loop of Fig. 1 to correspond to the Dirac matrices S, P, A, V, T and the latter to be dominated by the lowest $q\bar{q}$, S-wave states we have been considering. On the other hand, we cannot exclude that decreasing couplings of the higher resonances may eventually resum up to a significant effect, which would change the picture obtained by truncating the cross section to the lowest levels.

However, in all cases where this happens, like e.g. in deep inelastic lepton-hadron scattering, the final result reproduces what happens for free quarks and gluons. In our case, this would mean going over the Hagedorn temperature from the hadron into the quark and gluon gas, which is precisely what Fig. 8 seems to tell us.

VI.   CONCLUSIONS

The prediction that its formation is suppressed in quark-gluon plasma [5] makes the J/ψ a very interesting probe for a possible phase transition in heavy ion collisions. When the prediction was made, it was believed that J/ψ would suffer negligible absorption in the nuclear matter and in the hadron fireball formed during the collision. Subsequent studies showed that this is not the case and, for the probe to be efficient, one must determine in a reliable way the absorption of J/ψ from these two "conventional" sources. The absorption length of J/ψ in nuclear matter has been determined [2] from the the cross-section of $p + A \to J/\psi$+anything as a function of the nucleon number, A.

A method to estimate the absorption from the comoving particles was presented in a previous paper [1], under the simplified assumption that the comoving particles are a thermalised pion gas at temperature T. Starting from a calculation of the $\pi + J/\psi \to D^{(*)}\bar{D}^{(*)}$ cross-section based on the Constituent Quark Model [6], we showed that the absorption is potentially large and strongly temperature dependent. T itself can be determined by a fit to the data at low centrality, where the pion gas approximation could be better justified. Comparing the extrapolation to larger centralities with data, one could then judge if a further suppression is at work. The temperatures found in [1], $T \approx 200$ MeV, were rather on the high side but still in the right ball-park, a reassuring indication for a calculation completely based on microscopic parameters. On the other hand, for the method to be reliable, it is necessary to apply a better approximation than the simple pion gas.

In the present paper we have extended the calculation to the lowest-lying pseudoscalar and vector mesons, the $S-$wave $q\bar{q}$ states. Contributions from higher resonances like the A_1 and the other $P-$wave $q\bar{q}$ states could also be considered, at the price of increasing theoretical uncertainties, and should not change the picture. Vector mesons give
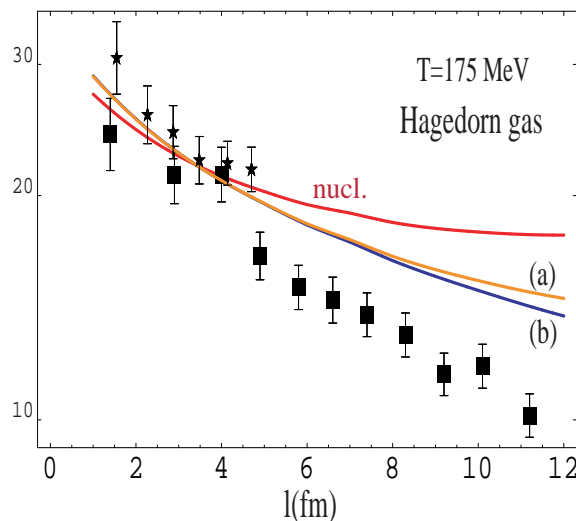
FIG. 8: The same as Fig. 7, without (a) or with (b) geometrical effects taken into account, using the energy-temperature dependence of the Hagedorn gas. The sharp rise of the degrees of freedom due to the vicinity of the Hagedorn temperature makes so that the temperature of the gas practically does not rise at all, the dissociation curve cannot become harder, and the prediction falls short from explaining the drop observed by NA50. Nuclear absorption alone is indicated by the upper curve.

substantial contributions to J/ψ dissociation, due to the higher multiplicities and because they are close or above threshold. As a consequence, we found a larger absorption in the heath bath at temperature T and a much lower range of temperatures to fit low centrality data, $T = 165 - 185$ MeV. This range agrees with the temperatures found from (i) particle abundances in ion collisions at freeze-out, (ii) the transition temperature found in lattice QCD calculations and (iii) the limiting temperature of a hadron gas [8, 9], as estimated from the experimental hadron level density.

In the range of temperatures considered, the number of active degrees of freedom is rapidly increasing, due to the excitation of more and more hadron levels (Fig. 5). This concept provides the ground for the existence of a limiting temperature in a hadron gas, the Hagedorn temperature. For the gas made by the comoving particles, the increase of the degrees of freedom "blocks" the temperature to the values observed for the low centrality events and prevents the opacity of the fireball to J/ψ to increase further. In fact, assuming a limiting temperature of about $170 - 180$ MeV from the outset, the decrease of J/ψ production observed by NA50 at large centralities cannot be explained with absorption by either the nuclear matter or the comoving particles, as shown in Fig. 8.

We cannot exclude that an infinite tower of higher resonances with decreasing couplings could eventually change the picture obtained by truncating the cross section to the lowest levels. Should this happen, however, we would expect the result to be close to that obtained by replacing the resonances with quarks and gluons, i.e. the situation one encounters in the QGP.

In conclusion, we believe that our calculation has produced a reliable estimate of J/ψ absorption in a hadron gas where only the lowest resonances are excited. It can agree marginally with the data at large centrality, at the expenses of accepting temperatures which are quite high ($T \approx 200$ MeV) with respect to the current theoretical estimates of the limiting hadron temperatures. On the other hand, should one introduce the limiting temperature as a boundary condition, it is impossible to fit the data at large centrality, thus providing considerable support to the idea that the suppression is produced by the quark-gluon plasma.

Further progress can be envisaged in several directions. Further measurements at low energy, aimed at resolving the experimental issue of the relative normalization of S-U vs. Pb-Pb data, would restrict the range of temperatures required at low centrality and allow for a more precise extrapolation with respect to what shown in Fig. 7. The onset of other possible signatures of the phase transition, such as strangeness production, should be correlated to the present signal, in centrality and energy. Finally, a quantitative calculation of the expected absorption curve, should the QGP be formed, would be of crucial importance.

---

[1] L. Maiani, F. Piccinini, A.D. Polosa, V. Riquer, Nucl. Phys. **A741**, 273 (2004).

[2] B. Alessandro *et al.* (NA50 Coll.), Nucl. Phys. **A715**, 679c (2003).

[3] J. Bjorken, Phys. Rev. **D27**, 140 (1983).

[4] M.C. Abreu *et al.*, Phys. Lett. **B450**, 456 (1999); M.C. Abreu *et al.*, Phys. Lett. **B477**, 28 (2000); For a discussion of the data taking with a ZDC, M.C. Abreu *et al.*, Phys. Lett. **B521**, 195 (2001).

[5] T. Matsui and H. Satz Phys. Lett. **B178**, 416 (1986); For a review, see e.g. R. Vogt, Phys. Rep. **310**, 197 (1999).

[6] A. Deandrea, N. Di Bartolomeo, R. Gatto, G. Nardulli and A.D. Polosa, Phys. Rev. **D58**, 034004 (1998); See also A.D. Polosa, Riv. Nuovo Cim. Vol. **23**, N. 11 (2000).

[7] see S. Matinyan and B. Müller, Phys. Rev. **C58**, 2994 (1998).

[8] R. Hagedorn, Nuovo Cim. Suppl. **3**, 147 (1965).

[9] J. Letessier and J. Rafelski, "Hadrons and Quark Gluon Plasma", Cambridge Monogr. Part. Phys. Nucl. Phys. Cosmol. **18** (2002).

[10] N. Cabibbo and G. Parisi, Phys. Lett. **59B**, 67 (1975).

[11] F. Karsch, "Lattice QCD at Nonzero Chemical Potential and the Resonance Gas Model", arXiv:hep-lat/0401031 and references therein.

[12] F. Antinori "Strangeness Report", in Quark 2004, arXiv:nucl-ex/0404032.

[13] http://na50.web.cern.ch/NA50/

[14] D. Ebert, T. Feldmann, R. Friedrich and H. Reinhardt, Nucl. Phys. **B434**, 619 (1995); D. Ebert, T. Feldmann and H. Reinhardt, Phys. Lett. **B388**, 154 (1996).

[15] T. Barnes, "Charmonium Cross Sections and the QGP", nucl-th/0306031.

[16] A. Deandrea, G. Nardulli and A.D. Polosa, Phys. Rev. **D68**, 034002 (2003); see also M. Bedjidian *et al.* "Hard Probes In Heavy Ion Collisions at the LHC: Heavy Flavor Physics", arXiv:hep-ph/0311048.

[17] A. Manohar and H. Georgi, Nucl. Phys. **B234**, 189 (1984).

[18] A. Deandrea, R. Gatto, G. Nardulli and A.D. Polosa, Phys. Lett. **B502**, 79 (2001).

[19] paper in preparation.

[20] D. Kharzeev, C. Lourenço, M. Nardi and H. Satz, Z. Phys. **C74**, 307 (1997).

[21] This range of temperatures is subject to a very tiny variation when the geometrical factor in Eq. (5) is taken to be $8/3\pi R$ instead of $3/4R$, i.e., if we consider a bidimensional (circle) fireball of radius R instead of a spherical one.

[22] The density of states with these values deviates from the best fit of Ref. [9] only above 1.5 GeV.